Incomplete Combustion: A Possible Cause of Combustion Instability

H.F. R. Schöyer*
Delft University of Technology, Delft, The Netherlands

The performance of and the combustion in solid-propellant rocket motors may be affected by characteristic length (L^*). For small characteristic lengths, the chamber pressure and characteristic velocity may be lower than in similar motors with larger L^*. Oscillatory combustion may take place if the L^* is small enough. In the past, L^* oscillations have been explained by an oscillatory heat feedback mechanism and subsequent oscillatory propellant pyrolysis. The same phenomena—i.e., lower chamber pressure, lower characteristic velocity, and oscillatory combustion—can also occur in liquid-propellant, hybrid, and airbreathing rocket motors. It is shown that these phenomena may be explained by assuming a finite reaction rate in the gas phase in combination with small residence times. Even if a constant burning rate or propellant mass flow rate is assumed, the coupling between the energy release in the gas phase and the residence time is sufficient to cause oscillatory combustion. A stability boundary criterion for solid-propellant rocket motors is derived and is found to be in agreement with experimental results.

Nomenclature

A = pre-exponential or frequency factor
A_t = nozzle throat area
A_1, A_2 = integration constants
a = burning rate coefficient
B = proportionality factor, defined in Eq. (19)
C_p = heat capacity at constant pressure
C_v = heat capacity at constant volume
C_1, C_2 = constants defined in Eqs. (15)
c = variable defined in Eq. (9b)
F = frequency
H = enthalpy
$H_k(T_0)$ = enthalpy of the solid propellant at its initial temperature
ΔH = heat of gasification
ΔH_f = heat of formation
K = concentration of reactants
K_n = ratio of burning surface area and nozzle throat area
k = reaction rate
L^* = characteristic length, V_c/A_t
M = molar mass
m = mass flow rate
N = variable defined in Eq. (22)
n = burning rate exponent
P = concentration of products
p = pressure
Q_w = rate of heat losses to the walls
q = rate of heat losses per mole
R = gas constant
R_0 = universal gas constant
r = burning rate
S = surface area
T = temperature
t = time
V = volume
v = velocity
β = temperature ratio
γ = ratio of specific heats
Γ = Vandenkerckhove function of γ
ϵ = incompleteness of combustion
η = dimensionless heat function
θ = activation temperature
κ = thermal diffusivity of the solid propellant
λ = proportionality factor for heat loss
ν = stoichiometric coefficient
ρ = density
τ^* = residence time

Subscripts and Superscripts

b = propellant
c = chamber
k = reactants
ℓ = at stability boundary
p = products
0 = initial conditions
∞ = adiabatic conditions while $L^* \to \infty$
$( )^0$ = at standard conditions
$( )'$ = perturbed quantity
$(\bar{\ })$ = mean (steady-state) quantity
$( )^{1/2}$ = positive root

Received April 20, 1982; revision received Nov. 9, 1982.

*Senior Faculty Member, Department of Aerospace Engineering; also Consultant National Defense Research Organization TNO. Member AIAA.

Introduction

SOLID-propellant rocket motors with small characteristic lengths may exhibit oscillatory combustion. In some cases the oscillation amplitudes grow rapidly, which may lead to a premature extinction of the motor (dp/dt extinguishment). Sometimes, such extinction is followed by reignition and a sequence of pressure buildup and oscillatory combustion, after which extinction may again occur. Decaying oscillations that finally die out have also been observed. It has even been observed[1,2] that during one single operation two different oscillations with different frequencies can occur (dual frequency). For very small characteristic lengths, a rapid pressure rise may be followed directly by extinction. In many cases, reignition takes place after a short period and the sequence of pressure buildup and extinction may repeat itself many times—a process known as chuffing.

Liquid-propellant rocket motors may also exhibit a low-frequency, bulk mode oscillation which appears to be closely related to the L^* or residence time of the motor.[3] Liljegren[4] has observed low-frequency (1-5 Hz) combustion instability in airbreathing, solid-propellant rocket motors. He noted that

the oscillatory amplitude decreased with increasing free-chamber volumes. These oscillations took place at characteristic lengths between 60 and 250 m. Similar observations have occasionally been made in hybrid rocket motors and there are indications that low-frequency oscillatory combustion instability may also occur in liquid-fuel ramjets.[5] These phenomena have in common that the frequency is usually below 300 Hz and that the oscillations are related to the characteristic length or residence time.

In solid-propellant rocket motors especially, the phenomenon has been studied extensively and is denoted as L^* instability. The oldest explanation is that of Akiba and Tanno.[6] The basic idea is that due to oscillatory combustion there is a fluctuating heat transfer into the propellant which superimposes an oscillation on the steady-state temperature profile in the pyrolizing solid propellant. Because the solid-propellant pyrolysis depends on the (fluctuating) surface temperature, the pyrolysis rate will also vary, causing a fluctuating mass flow into the combustion chamber. If this fluctuating mass flow is more or less in phase with the pressure fluctuation, the two effects may enhance each other (causing resonance) and may lead to oscillatory combustion. Sehgal and Strand[7] took a similar view and their approach, yielding very satisfactory results (especially at higher frequencies) has since been generally accepted. De Luca et al.[8] made an in-depth analysis of the nonlinear effects of an oscillating temperature profile in the solid propellant and its effect on propellant pyrolysis and subsequent combustion. However, the flame temperature was essentially estimated on the assumption that complete combustion is achieved in very short time frames. T'ien et al.[9] took a different approach when they specifically accounted for the possibility of small temperature fluctuations in the gas phase. However, the flame was again considered thin in comparison with the chamber length, which like De Luca's approach[8] implies very rapid gas-phase reactions. Caveny et al.[10] were among the first to consider incomplete gas-phase reactions as a factor that might contribute to combustion instability and ignition transients. They use many arguments similar to those pursued in the present studies, except that they do not specifically consider the variations in heat release and chemical composition resulting from the chemical kinetics being coupled with small residence times. As the frequency of the L^* oscillations has no relation whatsoever with any of the acoustic eigenfrequencies of the rocket motor, this type of oscillatory combustion has often been referred to as "nonacoustic." However, Oberg[11] and Culick[12] have shown that L^* oscillations can be regarded as a special solution of the acoustic wave equation.

Notwithstanding a continuous extension of the theory of low-frequency combustion instability to solid rocket propellants, discrepancies between theory and experiment remain, as perhaps best elucidated by Boggs and Beckstead.[2] They hypothesize that the oxidizer particle size might be a cause for some of the discrepancies mentioned. This might explain, for instance, the observed dual frequency. However, such a dual frequency has also been observed by Schöyer[1] for a double-base propellant that does not contain discrete oxidizer particles. In addition, one would expect that the nondimensional oscillatory frequency, $2\pi Fk/r^2$, is not strongly dependent on pressure. Schöyer[13] showed that this was not the case. In addition, it has been observed that during L^* oscillations in rocket motors the mean pressure may be lower than the expected equilibrium pressure. This is usually attributed to heat losses although in the absence of oscillations the agreement between the observed and expected pressures in the same device is usually better. By applying the measured (oscillatory) pressure history to the propellant burning rate law and calculating the amount of propellant that should have been consumed, one usually finds that actually a little less propellant has been consumed—indicating that the actual burning rate was somewhat lower than that suggested by the burning rate law.

Both Ramohalli and Schöyer have taken high-speed movies of L^* oscillations. These movies show very strong fluctuations in the light intensity during the oscillations. It is doubtful whether isentropic expansion and compression of the combustion gases can account for such strong variations in the emission of light. Such fluctuations in light intensity may be explained by the strong fluctuations in temperature. Temperature measurements during L^* oscillations have been made only occasionally. Eisel et al.[14] measured large temperature fluctuations (up to 500 K) during L^* oscillations. These fluctuations had a relative amplitude of 8-10%, which agrees fairly well with the relative amplitude of the pressure fluctuations. In addition, Eisel et al. observed that the gas-phase composition varied strongly during these oscillations. The observation that the composition of the combustion products can vary during bulk-mode instability confirms earlier observations by Price et al.[15] In Price's experiments, solid particles in the exhaust of an L^* burner were collected on a rotating drum and it was found that the composition of the exhaust varied with the fluctuation of the combustion pressure. During a pressure rise the exhaust contained predominantly aluminum oxide and during a pressure decrease ammonium perchlorate (AP) was also present in the exhaust, while at a pressure minimum aluminum was the main solid in the exhaust. The observations by Eisel et al.[14] and Price et al.[15] at least indicate that gas-phase processes are important and have to be accounted for.

In the present studies, the gas-phase processes are modeled by an elementary single-step forward reaction. Time-dependent solid-phase and solid-gas interface processes are ignored, although earlier work[6-10] indicates that these are important. Nevertheless, many of the phenomena observed during L^* or bulk-mode oscillations can be explained qualitatively with this model. The theory is not limited to solid-propellant rocket motors, but is also applicable to liquid-propellant and hybrid rocket motors, airbreathing rocket motors, and solid- and liquid-fuel ramjets. It is a slight extension of earlier work by Van Heerden[16] and Bilous and Amundson[17] on continuous-flow stirred tank reactors, whose theory—surprisingly enough—has been denoted as the C-star theory.[18] Finally, classical theory[6,7] has predicted a stability boundary in the $\ell n(p_c) - \ell n(L^*)$ plane with a slope of $-1/(2n)$, but experimental results[19] do not always agree very well with this observation. The present analysis predicts a stability boundary with a slope of $-1/(1-n)$.

Combustion Modeling

Only one gas-phase reaction is considered. It is assumed that gaseous reactants enter the combustion chamber and that a homogeneous mixture of products and reactants leaves the chamber through the nozzle. The reactants are either pyrolysis products of the solid propellant, vaporized liquid propellants, gaseous propellants, or a mixture of these. To avoid complications of an already intricate problem, neither the decomposition or vaporization process nor the heating of the reactants and products is considered in any detail. Instead, all of these processes are assumed to occur simultaneously and uniformly throughout the chamber. Therefore the model is one of volumetric gas-phase combustion reactions, analogous to the continuous-flow stirred tank reactor theory.[16-18] It is assumed that the mixture of gaseous reactants forms a mixture of gaseous products which may be expressed as,

$$\nu K \xrightarrow{k} P \tag{1}$$

It is assumed here that ν mole of K are required to form 1 mole of P. This implies that

$$\nu M_k = M_p \tag{2}$$

The reaction rate k is assumed to follow an Arrhenius relationship,

$$k = A\exp\{-\theta/T\} \tag{3}$$

Note that the activation temperature θ is a shorthand for the ratio of the activation energy and the universal gas constant.

Conservation of species requires

$$\frac{dK}{dt} + \frac{K}{\tau^*} + \nu k K = \frac{m}{M_k V_c} \tag{4}$$

$$\frac{dP}{dt} + \frac{P}{\tau^*} - kK = 0 \tag{5}$$

It is seen that a one-step, first-order reaction is assumed to represent the combustion reaction. The equation for conservation of energy for the combustion chamber of the rocket motor is

$$\frac{d}{dt}[(K+\nu P)H_k - (P+K)R_0T + P\Delta H_{f_p}] + [(K+\nu P)H_k + P\Delta H_{f_p}]/\tau^* - mH_k(T_0)/(M_k V_c) - Q_w/V_c = 0 \tag{6}$$

The heat losses to the walls (but not to the propellant) are indicated by Q_w. Simultaneously solving Eqs. (2-6) yields the concentration of the products and reactants and the temperature. Due to the highly nonlinear character of these equations, analytical solutions are not considered possible.

Steady-State Solutions

By assuming the enthalpy and heat transfer to be linear functions of the temperature, Eq. (6) for the steady state can be rewritten as

$$-\nu[H_k - H_k(T_0) - Q_w M_k/m]/\Delta H_{f_p} = \eta = 1/[1 + 1/(\nu k\tau^*)] \tag{7}$$

The left-hand side of Eq. (7) represents the heat required to arrive at a temperature T and the right-hand side expresses the amount of heat generated by the combustion process. While the left-hand side of Eq. (7) by good approximation is about linear with temperature, the right-hand side has a sigmoidal shape. The residence time may be expressed as,

$$\tau^* = L^*\sqrt{M_k(1+\nu k\tau^*)}/[\Gamma\sqrt{R_0T(1+k\tau^*)}] \tag{8}$$

which follows from the normal steady-state expression for the residence time[20] by replacing the pressure and the mean molecular weight with the reactants and product concentrations and substituting the steady-state form of Eq. (5) for the ratio of products and reactants.

For analytic purposes, an approximate expression for τ^* derived by "curve-fitting" Eq. (8),

$$\tau^* = c[kc\sqrt{\nu}(\sqrt{\nu}+1)+2]/[kc(\sqrt{\nu}+1)+2] \tag{9a}$$

with

$$c = L^*\sqrt{M_k}/(\Gamma\sqrt{R_0T}) \tag{9b}$$

will suffice, because for $kc \geq 100$ and $\nu \geq 0.2$ the accuracy of this approximation is better than 2.5%. The dimensionless heat release due to combustion is shown in Fig. 1 as a sigmoidal curve. The heat required is represented by the straight line. Solutions of Eq. (7) are the intersections of the straight line and the sigmoidal curve. Evidently there can be either no solutions or as many as three, not all of which have to be stable for steady-state situations.

In this paper we restrict ourselves to high-temperature solutions, as these are the ones that usually agree with the actual combustion in rocket motors. With increasing values of L^* (i.e., increasing values of τ^*) the sigmoidal curve shifts to the left, leading to higher combustion temperatures. This agrees with the observations of Feiler and Baker[21] who found experimentally that decreasing the rocket motor characteristic length would lead to lower chamber pressures and lower characteristic velocities. In fact, this is due to the τ^* becoming so small that the gases are expelled from the motor before the combustion has been completed.

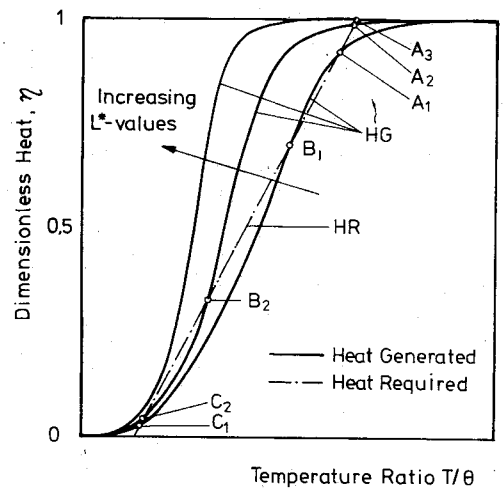

Fig. 1 Schematic representation of the solution of the combustion temperature in a rocket motor.

By enlarging the chamber volume of a rocket motor, and hence increasing its τ^*, heat losses may also be enlarged. Therefore, one may expect that the chamber pressure or the characteristic velocity achieves a maximum value with respect to L^*. If the rocket motor were to have adiabatic walls, this "maximum" would occur at $L^* \to \infty$. Defining the equilibrium pressure and temperature as those points at which their sensitivity to L^* has disappeared results in

$$p_\infty = \lim_{\frac{dp}{dL^*} \to 0} p, \qquad T_\infty = \lim_{\frac{dT}{dL^*} \to 0} T \tag{10}$$

It is convenient to use the ratios T/T_∞ and p/p_∞ instead of p and T. Note that the values will at most reach unity. By assuming that the heat loss to the chamber wall is proportional to the differences in the wall and gas temperatures, i.e., $Q_w = \lambda(T - T_0)$, the temperature at which the left-hand side of Eq. (7) equals zero may be written as

$$T_{\eta=0} = T_0 - \frac{\Delta H}{C_{p_s} - (\lambda M_k/m)}$$

At this fictitious reactant temperature, the heating and subsequent gasification of the propellant is not accompanied by any change in energy content. The fact that the heat of gasification ΔH is usually small and positive implies that $T_{\eta=0} < T_0 \approx 300$ K and hence $\beta = T_{\eta=0}/T \ll 1$.

Substituting Eq. (9) into Eq. (7), using the temperature ratio β, and subsequently solving for kc yields

$$kc = \left[\left(\frac{T}{T_\infty} - \beta\right)(1+\sqrt{\nu}) - \left(1 - \frac{T}{T_\infty}\right)2\nu + \left\{\left[\left(\frac{T}{T_\infty} - \beta\right) \times (1+\sqrt{\nu}) - \left(1 - \frac{T}{T_\infty}\right)2\nu\right]^2 + 8\left(\frac{T}{T_\infty} - \beta\right)\left(1 - \frac{T}{T_\infty}\right) \times (\nu\sqrt{\nu} + \nu^2)\right\}^{1/2}\right] \Big/ 2\left(1 - \frac{T}{T_\infty}\right)\nu\sqrt{\nu}(1+\sqrt{\nu}) \tag{11}$$

Equation (11) may be used to find the combustion temperature in relation to the characteristic length. For the high-temperature solution, i.e., $T/T_\infty \to 1$ or $(1 - T/T_\infty)^2 \ll 1$, Eq.

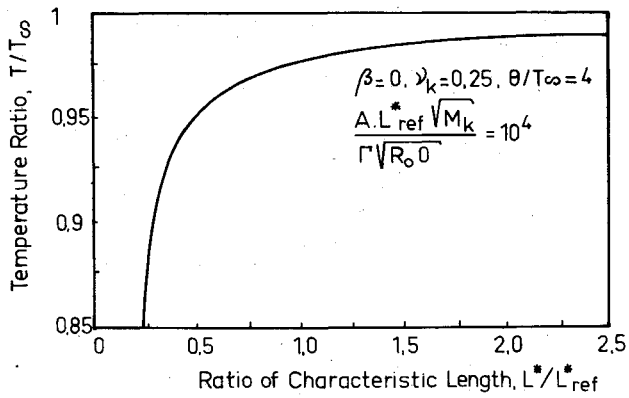

Fig. 2 Effect of characteristic length L^* on the combustion temperature T in a rocket motor.

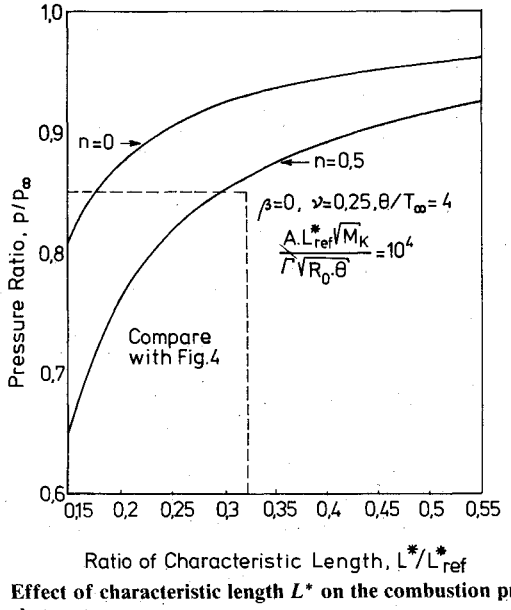

Fig. 3 Effect of characteristic length L^* on the combustion pressure p in a rocket motor.

(11) may be linearized to give

$$L^* = \frac{\Gamma\sqrt{R_0 T}}{A\exp\{-\theta/T\}\sqrt{\nu M_k}}\left[\frac{T/T_\infty - \beta}{\nu(1-T/T_\infty)} - \frac{2(1-\sqrt{\nu})}{1+\sqrt{\nu}}\right] \quad (12)$$

The solution of Eq. (12) is shown in Fig. 2. In this figure a reference value for L^* is used, L^*_{ref}, at which the temperature ratio T/T_∞ is assumed to be known.

Similarly, the effect of characteristic length on the chamber pressure may be derived. For a solid rocket motor, the mean flow (feed) is related to the pressure by "de Vieille's law,"

$$r = ap^n, \qquad n<1$$

For a liquid rocket motor, the feed is in effect independent of the pressure, i.e., $n=0$. Therefore, the chamber pressure may be expressed in general as

$$p^{1-n} = \frac{\rho_b a S_b \sqrt{R_0 T_\infty}}{\sqrt{M_k}(1-\beta)\Gamma A_t}\sqrt{\frac{T}{T_\infty}\left(1+\frac{1-\nu}{\nu}\frac{T}{T_\infty}-\frac{\beta}{\nu}\right)} \quad (13)$$

Assuming that $p=p_\infty$ for $T=T_\infty$, one obtains after linearization and neglecting terms of order $(1-T/T_\infty)^2$ and higher

$$\left(\frac{p}{p_\infty}\right)^{1-n} = \frac{\nu-\beta}{2(1-\beta)} + \frac{T}{T_\infty}\frac{2-\nu-\beta}{2(1-\beta)} \quad (14)$$

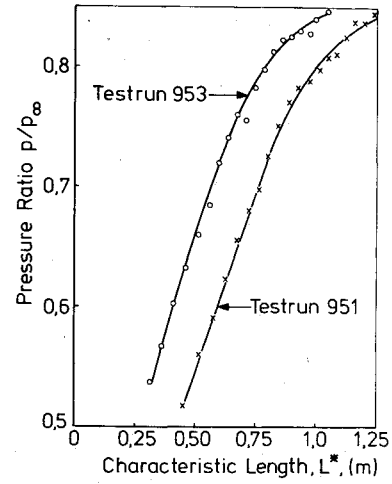

Fig. 4 Observed ratio of mean pressure $\bar{p}$ and ideal mean pressure p_∞ vs characteristic length L^* during L^* oscillations.

From Eqs. (12) and (14) a relation between p/p_∞ and L^* may be derived. This is shown in Fig. 3. Indeed, it is seen that for low values of L^*, the actual chamber pressure is lower than that which would be expected on grounds of complete combustion. This theoretical curve may be compared with the experimental data obtained by De Boer et al.[22] These results are shown in Fig. 4. Because a very small inaccuracy in the measured, or calculated, distance from the propellant surface to the nozzle will lead to a rather large difference in L^*, the fact that both experimentally observed curves do not coincide may be due to experimental inaccuracies. The shape of the curves, however, agrees fairly well with the shape of the curves in Fig. 3.

It is obvious from Fig. 3 that liquid-propellant rocket motors, where $n\approx 0$ are affected less by L^* than their solid propellant counterparts. Linearizing Eq. (12) in terms of $(\theta/T_\infty)(1-T/T_\infty)$ leads to a direct relationship between L^* and p/p_∞ of the form

$$L^* = \{C_1/[1-(p/p_\infty)^{1-n}] + C_2\}\frac{\Gamma\sqrt{R_0\theta}}{A\sqrt{\nu M_k}}\sqrt{\frac{T_\infty}{\theta}}e^{\theta/T_\infty} \quad (15a)$$

where

$$C_1 = \frac{2-\nu-\beta}{2\nu} \quad (15b)$$

and

$$C_2 = \frac{1-\beta}{2\nu}\left(2\frac{\theta}{T_\infty}-1\right) - \frac{1}{\nu} - \frac{2(1-\sqrt{\nu})}{1+\sqrt{\nu}} \quad (15c)$$

A regression analysis for the experimentally obtained L^*-pressure curves by De Boer et al.[22] shows correlation coefficients of 0.9977 and 0.9931, respectively, supporting the validity of the functional relationship as expressed by Eqs. (15).

These curves have been obtained with a double-base propellant in small test motors. Qualitatively, the curves agree very well with the curves obtained by Feiler and Baker[21] with liquid-propellant test motors, supporting the hypothesis that incomplete combustion due to small residence times in combination with finite reaction rates causes the observed low chamber pressures. It should be recalled that the temperature ratio β slightly increases with increasing characteristic lengths due to larger heat losses. This leads to the optimum value of L^* observed by Feiler and Baker.[21]

Time-Dependent Solutions

Due to their highly nonlinear character, Eqs. (2-9) cannot be solved analytically. It is possible, however, to investigate small variations around a stationary situation. To this end, all of the relevant variables are written in the form $\psi=\bar{\psi}+\psi'$ with $(\psi'/\bar{\psi})^2 \ll 1$, so that terms of order $(\psi'/\bar{\psi})^2$ and higher may be neglected. For the present, it is assumed that the mass flow into the combustion chamber is constant. Notwithstanding this important restriction, pressure and temperature oscillations may occur.

Putting $q_w = Q_w M_k/m = \lambda(T_w - T)/m$, the following set of equations describing the behavior of small perturbations around a stationary situation:

$$\left[C_v T - R_0 T \frac{1-\nu}{\nu}\eta\right]\frac{\mathrm{d}}{\mathrm{d}t/\tau^*}\left(\frac{T'}{T}\right) + \left[C_p T + \frac{\theta}{T}(H_k^0(T_0) - H_k) + q_w\left(\frac{\theta}{T}-1\right)\right]\frac{T'}{T} - R_0 T(1-\eta)\frac{\mathrm{d}}{\mathrm{d}t/\tau^*}\left(\frac{K'}{K}\right) + [H_k(T_0) - H_k + q_w]\frac{K'}{K} - R_0 T\frac{\eta}{\nu}\frac{\mathrm{d}}{\mathrm{d}t/\tau^*}\left(\frac{P'}{P}\right) = 0 \tag{16}$$

$$\frac{\mathrm{d}}{\mathrm{d}t/\tau^*}\left(\frac{K'}{K}\right) + \frac{K'/K}{1-\eta} - \frac{\tau^{*\prime}}{\tau^*} + \frac{\eta}{1-\eta}\frac{\theta}{T}\frac{T'}{T} = 0 \tag{17}$$

$$\frac{\mathrm{d}}{\mathrm{d}t/\tau^*}\left(\frac{P'}{P}\right) + \frac{P'}{P} - \frac{\tau^{*\prime}}{\tau^*} - \frac{K'}{K} - \frac{\theta}{T}\frac{T'}{T} = 0 \tag{18}$$

where

$$\tau^{*\prime}/\tau^* = BT'/T \tag{19}$$

The bars indicating steady-state solutions have been dropped. Expressing the product concentration P in pressure p slightly simplifies this set of equations. The equation relating p to the product concentration P is simply the equation of state,

$$p = R_0 T(P+K)$$

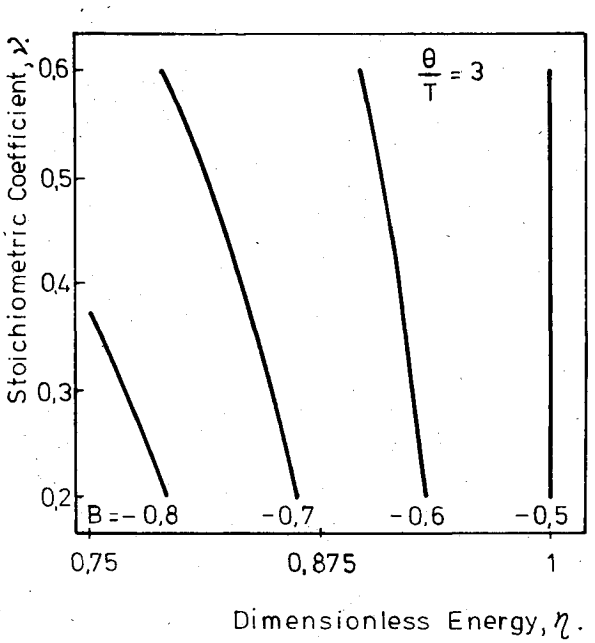

Fig. 5 Residence time parameter B as a function of dimensionless energy η and stoichiometric coefficient ν.

The equation for the pressure perturbation then becomes

$$\frac{\mathrm{d}}{\mathrm{d}t/\tau^*}\frac{p'}{p} + \frac{p'}{p} - \frac{\mathrm{d}}{\mathrm{d}t/\tau^*}\frac{T'}{T} - \left[B+1+\frac{\theta}{T}\frac{(1-\nu)\eta}{\nu+\eta(1-\nu)}\right]\frac{T'}{T} - \frac{\eta(1-\nu)}{\nu+\eta(1-\nu)}\frac{K'}{K} = 0 \tag{20}$$

Similarly the product concentration may be replaced by the pressure in Eq. (16).

This set of three coupled first-order differential equations may be replaced by one equation of third order in either of the variables. For our present purposes the pressure fluctuation is taken to be the primary variable of interest. This yields

$$\left[\frac{\eta(1-\nu)}{\nu} - \frac{\gamma}{\gamma-1}N\right]\frac{\mathrm{d}^3 p'/p}{\mathrm{d}t/\tau^{*3}} + \left\{N\left[\frac{\theta}{T}\frac{\eta}{\nu}\left(1-\nu-\frac{\Delta H_{f_p}}{R_0 T}\right) + \frac{q_w}{R_0 T} - \frac{3-2\eta}{1-\eta}\frac{\gamma}{\gamma-1}\right] + B\frac{\eta}{\nu}(1-\nu) + \frac{2-\eta}{1-\eta} \times \frac{\eta}{\nu}(1-\nu)\right\}\frac{\mathrm{d}^2 p'/p}{\mathrm{d}t/\tau^{*2}} + \left\{N\left[B\left(1-\nu-\frac{\Delta H_{f_p}}{R_0 T}\right)\frac{\eta}{\nu} + \frac{\theta}{T}\frac{\eta}{\nu}\left(1-\nu-2\frac{\Delta H_{f_p}}{R_0 T}\right) - \frac{\gamma}{\gamma-1}\frac{3-\eta}{1-\eta} + \frac{2-\eta}{1-\eta}\frac{q_w}{R_0 T}\right] + B\left(\frac{\eta}{1-\eta}\frac{1-\nu}{\nu}\right) + \frac{\eta}{1-\eta}\frac{1-\nu}{\nu}\right\}\frac{\mathrm{d}p'/p}{\mathrm{d}t/\tau^*} - \left[N\left(\frac{\theta}{T}+B\right)\frac{\eta}{\nu}\frac{\Delta H_{f_p}}{R_0 T} + \left(\frac{\gamma}{\gamma-1} - \frac{q_w}{R_0 T}\right)\frac{1}{1-\eta}\right]\frac{p'}{p} = 0 \tag{21}$$

and

$$N(\nu,\eta) = \frac{(1-\nu)\eta}{\nu+\eta(1-\nu)} \tag{22}$$

If instead of the relative pressure fluctuation, the relative temperature fluctuation is taken as the primary variable, a similar differential equation results; hence the relative temperature fluctuation is the same as the relative pressure fluctuation. This is an important result, but it is not affected by the simplifications which have to be made to obtain the approximate analytical solutions of Eq. (21).

Analytical solutions of this equation are difficult to obtain. However, by neglecting the variation in residence time, i.e., putting $B=0$, analytical solutions to Eq. (21) can be obtained. From Eqs. (8) and (19), by neglecting terms of second order and higher, it follows that

$$B = -\frac{(\nu-\nu\eta+1) + (\theta/T)\eta(1-\eta)(1-\nu)}{2\nu(1-\eta)^2 + (\nu+3)\eta(1-\eta) + 2\eta^2} \tag{23}$$

and for $\eta \to 1$, $B \to -\frac{1}{2}$. Figure 5 shows lines for the constant values of B vs ν and η. For $\eta > 0.9$, one sees that $-0.6 \lesssim B \lesssim -0.5$. For smaller values of η, i.e., when there is a severe incompleteness of combustion, B may decrease slowly but its absolute value remains small in comparison with the other terms in Eq. (21), although it is not negligible. By putting $B=0$, one obtains an approximate analytical solution which it is hoped will reveal at least some important physical features of the real problem. In fact, putting $B=0$ comes down to the assumption that, although there are variations in the pressure, temperature, and composition, the residence time is substantially constant. With this simplification, Eq. (21) may be

written as

$$\left[\frac{\mathrm{d}}{\mathrm{d}t/\tau^*}+1\right]\left\{\left(\frac{\eta(1-\nu)}{\nu}-\frac{\gamma}{\gamma-1}N\right)\frac{\mathrm{d}^2p'/p}{\mathrm{d}t/\tau^{*2}}+\left[N\left\{\frac{\theta}{T}\frac{\eta}{\nu}\left(1-\nu-\frac{\Delta H_{f_p}}{R_0T}\right)+\frac{q_w}{R_0T}-\frac{\gamma}{\gamma-1}\frac{2-\eta}{1-\eta}\right\}+\frac{\eta}{1-\eta}\frac{1-\nu}{\nu}\right]\frac{\mathrm{d}p'/p}{\mathrm{d}t/\tau^*}\right.$$

$$\left.-N\left(\frac{\theta}{T}\frac{\eta}{\nu}\frac{\Delta H_{f_p}}{R_0T}+\frac{\gamma}{\gamma-1}\frac{1}{1-\eta}-\frac{1}{1-\eta}\frac{q_w}{R_0T}\right)\frac{p'}{p}\right\}=0 \tag{24}$$

The solution associated with $\mathrm{d}/(\mathrm{d}t/\tau^*)+1=0$ represents the evacuation of the chamber and yields an exponentially decaying function that is not of interest here.

The solutions to be associated with the second-order differential equation are more interesting. We will pursue the high-temperature solutions, i.e., those that correspond with the intersection of the straight line for the heat required curve and the sigmoidal curve for the heat generated for large T and $\eta\to1$ (points $A_{1,2,3}$ in Fig. 1), because it is this solution that usually agrees with the actual situation in a rocket motor. In that case $\epsilon=1-\eta$ and $\epsilon^2\ll1$ is assumed so that terms of order ϵ^2 and higher may be neglected. By Eq. (7) the incompleteness of the combustion is directly related to the reaction rate and the residence time ($1/\epsilon=1+\nu k\tau^*$). The second-order differential equation for the pressure perturbation may be written as

$$\epsilon\left[\frac{1}{\nu}-\frac{\gamma}{\gamma-1}\right]\frac{\mathrm{d}^2p'/p}{\mathrm{d}t/\tau^{*2}}+\left\{\epsilon\left[\frac{\theta}{T}\frac{1}{\nu}\left(1-\nu-\frac{\Delta H_{f_p}}{R_0T}\right)+\frac{q_w}{R_0T}-\nu-\frac{1}{\gamma-1}\right]+\frac{1}{\nu}-\frac{\gamma}{\gamma-1}\right\}\frac{\mathrm{d}p'/p}{\mathrm{d}t/\tau^*}$$

$$-\left[\epsilon\frac{\theta}{T}\frac{1}{\nu}\frac{\Delta H_{f_p}}{R_0T}+\frac{\gamma}{\gamma-1}-\frac{q_w}{R_0T}\right]p'/p=0 \tag{25}$$

and obviously

$$\frac{p'}{p}=A_1\exp\left[\left\{-\frac{1}{2\epsilon}-\frac{\frac{\theta}{T}\frac{1}{\nu}\left(1-\nu-\frac{\Delta H_{f_p}}{R_0T}\right)+\frac{q_w}{R_0T}-\nu-\frac{1}{\gamma-1}}{2\left(\frac{1}{\nu}-\frac{\gamma}{\gamma-1}\right)}+\frac{1}{2\epsilon}\left(1+2\epsilon\frac{\frac{\theta}{T}\frac{1}{\nu}\left(1-\nu-\frac{\Delta H_{f_p}}{R_0T}\right)-\frac{q_w}{R_0T}-\nu+1+\frac{\gamma}{\gamma-1}}{\frac{1}{\nu}-\frac{\gamma}{\gamma-1}}\right)^{1/2}\right\}\frac{t}{\tau^*}\right]$$

$$+A_2\exp\left[\left\{-\frac{1}{2\epsilon}-\frac{\frac{\theta}{T}\frac{1}{\nu}\left(1-\nu-\frac{\Delta H_{f_p}}{R_0T}\right)+\frac{q_w}{R_0T}-\nu-\frac{\gamma}{\gamma-1}}{2\left(\frac{1}{\nu}-\frac{\gamma}{\gamma-1}\right)}-\frac{1}{2\epsilon}\left(1+2\epsilon\frac{\frac{\theta}{T}\frac{1}{\nu}\left(1-\nu-\frac{\Delta H_{f_p}}{R_0T}\right)-\frac{q_w}{R_0T}-\nu+1+\frac{\gamma}{\gamma-1}}{\frac{1}{\nu}-\frac{\gamma}{\gamma-1}}\right)^{1/2}\right\}\frac{t}{\tau^*}\right] \tag{26a}$$

This equation expresses how a small pressure perturbation p' about the "high-temperature solution" in the combustion chamber of a rocket motor will develop in time due to finite reaction rates and finite residence times.

For $\epsilon\to0$ and

$$1+2\epsilon\frac{\frac{\theta}{T}\frac{1}{\nu}\left(1-\nu-\frac{\Delta H_{f_p}}{R_0T}\right)-\frac{q_w}{R_0T}-\nu+1+\frac{\gamma}{\gamma-1}}{\frac{1}{\nu}-\frac{\gamma}{\gamma-1}}>0$$

i.e., for a nearly completed combustion and a positive discriminant, Eq. (26a) may also be written as

$$p'/p=A_1\exp\left[\frac{\frac{\gamma}{\gamma-1}-\frac{q_w}{R_0T}}{\frac{1}{\nu}-\frac{t}{\gamma-1}}\frac{t}{\tau^*}\right]+A_2\exp\left[\left\{-\nu k+\frac{\frac{\theta}{T}\frac{1}{\nu}\left(1-\nu-\frac{\Delta H_{f_p}}{R_0T}\right)-\frac{1}{\nu}+\nu+\frac{\gamma+2}{\gamma-1}}{\left(\frac{1}{\nu}-\frac{\gamma}{\gamma-1}\right)\tau^*}\right\}t\right] \tag{26b}$$

It should be recalled that γ represents the ratio of the specific heats of the reactants. In the case of pyrolizing solid propellants, the reactants may contain large molecules leading to small values of γ. Therefore, $\gamma/(\gamma-1)$ may be rather large, while on the other hand the stoichiometric coefficient may be estimated to lie somewhere between 0.2 and unity.

So, for many propellants $1/\nu<\gamma/(\gamma-1)$; moreover, $\gamma/(\gamma-1)>q_w/R_0T$, as otherwise more heat would be extracted than is stored in the combustion gases. Therefore, the first exponential will be negative and the second exponential will contain a large reaction rate. In addition, the second term of the second exponential in most cases will be negative, the denominator usually being assumed to be negative, while for the same reason the numerator is positive. Therefore, for a positive discriminant, perturbations will die out exponentially.

Equation (26) also allows for oscillatory solutions. These will occur if

$$\frac{1}{2\epsilon}<\frac{\frac{1}{\nu}\frac{\theta}{T}\left(1-\nu-\frac{\Delta H_{f_p}}{R_0T}\right)-\frac{q_w}{R_0T}-\nu+1+\frac{\gamma}{\gamma-1}}{\frac{\gamma}{\gamma-1}-\frac{1}{\nu}} \tag{27}$$

i.e., for a negative discriminant.

The oscillatory frequency F follows from

$$F=\frac{1}{4\pi\epsilon\tau^*}\left[2\epsilon\frac{\frac{\theta}{T}\left(1-\nu-\frac{\Delta H_{f_p}}{R_0T}\right)-\frac{\nu q_w}{R_0T}+\frac{\nu\gamma}{\gamma-1}-\nu(1-\nu)}{\frac{\nu\gamma}{\gamma-1}-1}-1\right]^{1/2} \tag{28}$$

Decaying amplitudes occur if

$$\frac{\frac{1}{\nu}\frac{\theta}{T}\left(1-\nu-\frac{\Delta H_{f_p}}{R_0T}\right)-\frac{q_w}{R_0T}-\nu+1+\frac{\gamma}{\gamma-1}}{\frac{\gamma}{\gamma-1}-\frac{1}{\nu}}>\frac{1}{2\epsilon}$$

$$>\frac{\frac{\theta}{T}\frac{1}{\nu}\left(1-\nu-\frac{\Delta H_{f_p}}{R_0T}\right)+\frac{q_w}{R_0T}-\nu-\frac{1}{\gamma-1}}{2\left(\frac{\gamma}{\gamma-1}-\frac{1}{\nu}\right)} \tag{29a}$$

The amplitudes remain constant if

$$\frac{1}{\epsilon}=\frac{\frac{\theta}{T}\frac{1}{\nu}\left(1-\nu-\frac{\Delta H_{f_p}}{R_0T}\right)+\frac{q_w}{R_0T}-\nu-\frac{1}{\gamma-1}}{\frac{\gamma}{\gamma-1}-\frac{1}{\nu}} \tag{29b}$$

Oscillatory combustion with growing amplitudes occurs if

$$\frac{1}{\epsilon}<\frac{\frac{\theta}{T}\frac{1}{\nu}\left(1-\nu-\frac{\Delta H_{f_p}}{R_0T}\right)+\frac{q_w}{R_0T}-\nu-\frac{1}{\gamma-1}}{\frac{\gamma}{\gamma-1}-\frac{1}{\nu}} \tag{29c}$$

So increasing the value of ϵ, starting with stable combustion (i.e., combustion without oscillations), will first decrease the mean combustion temperature and pressure. Subsequently, the inequality of Eq. (27) will apply and any perturbation will lead to oscillatory combustion dampening out exponentially. Thereafter, when Eq. (29b) is satisfied, the oscillations will continue at the same amplitude level. Finally, still further increasing the value of ϵ will lead to oscillatory combustion with exponentially growing amplitudes.

Increasing values of ϵ correspond to decreasing values of the residence time of the rocket motor, i.e., to decreasing values of the characteristic length L^*.

According to this analysis, incomplete combustion that is due to a combination of finite reaction rates and short residence times may cause oscillatory combustion. In that case, the mean chamber pressure and temperature will be lower than their respective equilibrium values, which have been observed during L^* oscillations in solid-propellant rocket motors. A measure of the completeness of combustion is the dimensionless heat parameter η. For $\eta<1$ combustion is incomplete. The actual combustion pressure and temperature for a given propellant depends solely on the completeness of combustion. According to this analysis the relative temperature oscillations should be the same as the relative pressure oscillations. Also, these oscillations must be accompanied by fluctuations in the composition of the gases in the combustion chamber. The measurements of Eisel et al.[14] suggest that the relative temperature and pressure oscillations can be of the same magnitude. Variations in the composition of the combustion gases and the exhaust have been observed by Eisel et al.[14] and Price et al.[15]

Stability Boundary

The point at which, during L^* oscillations with decaying amplitudes, the oscillations merge with the noise of the signal has often been taken as a locus of the stability boundary[1,23] in the L^*-p plane. Strand[19] takes the point where the first (growing) oscillations appear (onset of instability, point OI) as a locus of the stability boundary. In the first case, due to the consumption of propellant, the residence time will have already increased with respect to its value at OI, and this increase may strongly depend on the particular experiment. For that reason, Strand's definition may be the better one.

For both definitions, one usually finds an approximately straight line, with a negative slope, in the $\ell n\, L^*$-$\ell n p$ plane. The slope of the OI curve, however, is the steeper one.

According to "classical theory,"[19] this slope should equal $-1/(2n)$ (n being the burning rate exponent). It should be noted that when the pressure is on the horizontal axis and L^* on the vertical axis, the slope is $-2n$. If L^* instability indeed results from incomplete combustion, Eq. (29b) may be regarded as an equation for the stability boundary, which may also be interpreted as

$$\nu\tau_\ell^* A\exp\{-\theta/T_\ell\}=\text{const} \tag{30a}$$

$$\eta_\ell=\text{const}<1 \tag{30b}$$

Because the combustion temperature T during incomplete combustion depends solely on η, Eq. (30a) may be simplified to

$$\tau_\ell^*=\text{const} \tag{30c}$$

or equivalently

$$\tau_\ell^*=p_\ell^{1-n}L_\ell^*/(\rho_b R_\ell T_\ell a K_n) \tag{31}$$

It is evident that Eqs. (30) and (31) are steady-state equilibrium conditions at a residence time and combustion temperature that agree with L^* oscillations at a constant amplitude.

Logarithmic differentiation of Eq. (31) yields the slope of the stability boundary

$$(1-n)\frac{d\ell n p_\ell}{d\ell n L_\ell^*}-\frac{d\ell n K_n}{d\ell n L_\ell^*}=-1 \tag{32a}$$

and in the case where K_n is constant, as with most L^* burners,

$$\frac{d\ell n p_\ell}{d\ell n L_\ell^*}=\frac{-1}{1-n} \tag{32b}$$

Figure 6 shows the points on OI that have been obtained from experiments with ANP-2830 composite propellant in 10 and 5 cm i.d. L^* burners. These experiments have been reported before.[1,13]

In the appropriate pressure range, the propellant burn rate exponent is $n\approx 0.36$, which would imply a slope $d\ell n p/d\ell n L^*\approx -1.5625$. This agrees favorably with the observed slopes (-1.43 and -1.57). However, "classical theory" predicts a slope $d(\ell n p)/d(\ell n L^*)=-1/(2n)\approx -1.39$. Therefore, the results reported here are not decisive for discriminating between the two theories. The scatter in the data is believed to be caused primarily by inaccuracies in the L^* values (any inaccuracy in the distance between the burning surface and the nozzle end plate is reflected by the about 100 times larger inaccuracy in the L^* values).

Unfortunately, it was not possible to check the theory with Strand's data[19] because in his experiments the grains burned regressively and, hence, K_n changed with L^*, while Kumar's data[23] did not use OI to correlate the stability boundary.

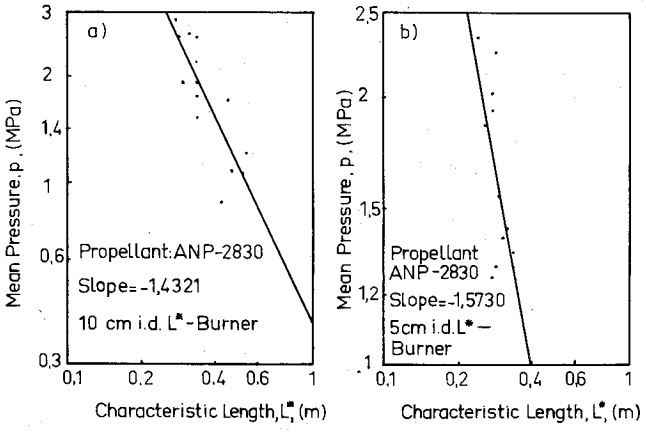

Fig. 6 Observed OI-line for ANP-2830 composite propellant: a) 10 cm i.d. L^* burner, b) 5 cm i.d. L^* burner.

It has often been observed that the loci of the points of dp/dt extinguishment run parallel to the stability boundary. As dp/dt extinguishment will occur only for continuously growing amplitudes, this implies a severe "incompleteness of combustion." One could assume that this is described by Eq. (29c), implying a similar slope for the "dp/dt extinguishment boundary."

Discussion and Conclusions

A hypothesis has been proposed that relates L^* instability to incomplete combustion due to finite (gas-phase) reaction rates and short residence times. Most of the supporting evidence is still of a qualitative nature, although some experimental results agree reasonably well with the theory. The observations of Feiler and Baker,[21] that mean pressure and temperature in liquid-propellant rocket motors may not achieve their expected equilibrium values for small L^*, may well be explained by the present theory. The theory also explains the observed large variations in light intensity during L^* oscillations. The small-amplitude, high-frequency oscillations (dual frequency)[1,2] may perhaps be interpreted as oscillations around the lower stable equilibrium solution (points C in Fig. 1). It is intended to pursue these and other features in more detail in the future. Further details which require thorough investigation are the solid-phase processes and the constitution of propellant pyrolysis products. Many observations[22,24] reveal a frequency and/or amplitude modulation during L^* oscillations which might perhaps be explained by oscillatory propellant pyrolysis, but which deserve a more detailed analysis in the light of the proposed mechanism.

Being of a general nature, the proposed mechanism may have far-reaching implications for other combustion systems such as solid- and liquid-fuel ramjets and hybrid rocket motors.

Acknowledgments

The author is much indebted to A. Paauw of the Laboratory of Thermal Power Engineering of DUT (presently at Shell Internationale Petroleum Mij, MF-New Plant Development) who drew his attention to the theory of continuous-flow stirred reactors after watching a movie of the large fluctuations in light intensity (and color) associated with L^* oscillations.

References

[1] Schöyer, H.F.R., "Results of Experimental Investigations of the L^* Phenomenon," *Journal of Spacecraft and Rockets*, Vol. 17, May-June 1980, pp. 200-207.

[2] Boggs, T. L. and Beckstead, M. W., "Failure of Existing Theories to Correlate Experimental Nonacoustic Combustion Instability Data," *AIAA Journal*, Vol. 8, April 1970, pp. 626-631.

[3] Harrje, D. T. and Reardon, F. H. (Eds.), "Liquid Propellant Rocket Combustion Instability," NASA SP-194, 1972.

[4] Liljegren, T., "Combustion of Fuel-Rich HTPB-Propellants with Ammonium Perchlorate as Oxidizer," *Proceedings of the Internationale Jahrestagung 1979*, Fraunhofer Institut für Treib- und Explosivstoffe, ICT, Karlsruhe, FRG, 1979, pp. 363-376.

[5] Crump, J. E. and Schadow, K. C., personal communication, Autumn 1981.

[6] Akiba, R. and Tanno, M., "Low Frequency Instability in Solid Propellant Rocket Motors," *Proceedings of the First Symposium (International) on Rockets and Astronautics*, Tokyo, 1959, Yokendo, Tokyo, 1960, pp. 74-82.

[7] Sehgal, R. and Strand, L. D., "A Theory of Low-Frequency Combustion Instability in Solid Rocket Motors," *AIAA Journal*, Vol. 2, April 1964, pp. 696-702.

[8] De Luca, L., Galfetti, L., Riva, G., and Tabacco, U., "Unstable Burning of Thin Solid Propellant Flames," AIAA Paper 80-1126, 1980.

[9] T'ien, J. S., Sirignano, W. A., and Summerfield, M., "Theory of L-star Combustion Instability with Temperature Oscillations," *AIAA Journal*, Vol. 8, Jan. 1970, pp. 120-126.

[10] Caveny, L. H., Battista, R. A., and Summerfield, M., "Pressure Transients of Solid Rockets with Slow Gas Phase Reaction Times," AIAA Paper 73-1301, Nov. 1973.

[11] Oberg, C. L., "Combustion Instability: The Relationship Between Acoustic and Nonacoustic Instability," *AIAA Journal*, Vol. 6, Feb. 1968, pp. 265-271.

[12] Culick, F.E.C., "Some Nonacoustic Instabilities in Rocket Chambers Are Acoustic," *AIAA Journal*, Vol. 6, July 1968, pp. 1421-1423.

[13] Schöyer, H.F.R., "Low Frequency Oscillatory Combustion: Experiments and Results," *Solid Rocket Motor Technology*, AGARD CP 259, 1979, pp. 25-1-25-16.

[14] Eisel, J. L., Ryan, N. W., and Baer, A. D., "Combustion of NH_4CLO_4-Polyurethane Propellants: Pressure, Temperature, and Gas-Phase Composition Fluctuations," *AIAA Journal*, Vol. 10, Dec. 1972, pp. 1655-1661.

[15] Price, E. W., Rice, D. W., and Crump, J. E., "Low-Frequency Combustion Instability of Solid Rocket Propellants, 1 May 1963-31 May 1964," U.S. Naval Ordnance Test Station, China Lake, Calif., Technical Progress Rept. 360, NOTS TP 3524, 1964.

[16] Van Heerden, C., "Autothermic Processes, Properties and Reactor Design," *Industrial and Engineering Chemistry*, Vol. 45, June 1953, pp. 1242-1247.

[17] Bilous, O. and Amundson, N. R., "Chemical Reactor Stability and Sensitivity," *AIChE Journal*, Vol. 1, No. 4, 1955, pp. 513-521.

[18] Aris, R., "Elementary Chemical Reactor Analysis," 1st ed., Prentice-Hall, Englewood Cliffs, N.J., 1969, p. 156.

[19] Strand, L. D., "Summary of a Study of the Low-Pressure Combustion of Solid Propellants," Jet Propulsion Laboratory, California Institute of Technology, Pasadena, Tech. Rept. 32-1242, 1968.

[20] Cornelisse, J. W., Schöyer, H.F.R., and Wakker, K. F., *Rocket Propulsion and Spaceflight Dynamics*, 1st ed., Pitman, London, 1979, p. 121.

[21] Feiler, C. E. and Baker, Jr. L., "A Study of Fuel-Nitric Acid Reactivity," NACA RM E56A19, 1956.

[22] De Boer, R. S., Schöyer, H.F.R., and Wolff, H., "Results of L^* Instability Experiments with Double Base Rocket Propellants II," Delft University of Technology, Dept. of Aerospace Engineering/Technological Laboratory TNO, Delft/Rijswijk, the Netherlands, Rept. LR-252/TL R 3050-II, 1977.

[23] Kumar, R N., "Some Experimental Results on the L-Star Instability of Metallized Composite Propellants," AIAA Paper 75-226, Jan. 1975.

[24] Schöyer, H.F.R., "Report on Low-Frequency Oscillatory Combustion Experiments," California Institute of Technology, Pasadena, Feb. 1971.